

# LONG-TERM CORROSION FATIGUE CRACK PROPAGATION BEHAVIOR IN WELDED MEMBERS

Masahiro SAKANO\*, Toshio NISHIMURA\*\*  
and Takeshi KOGURE\*\*\*

Fatigue crack propagation tests are conducted in air and in the wet condition of 3% NaCl solution using plate-type specimens with longitudinal weldments in order to investigate the effect of corrosive environment on the long-term fatigue crack propagation behavior in welded members. In corrosive environment, fatigue cracks can be propagated in the smaller  $\Delta K$  region, and no threshold behavior is observed. The  $da/dN - \Delta K$  relationship of welded members in corrosive environment can be represented by the constant value in the region of  $\Delta K$  smaller than the threshold value in air.

*Keywords* : corrosion fatigue, long-term crack propagation, welded member, residual stress, threshold behavior

## 1. INTRODUCTION

In recent years, a number of steel bridges have been constructed or planned across the straits, in the bay area, and in the cold districts where antifreezing agents are necessary in winter. On one hand, as years go by, numbers of existing steel bridges have been affected at least in some part by corrosive environments in the hot and humid climate. It is of immediate importance to grasp the fatigue behavior of steel bridges in corrosive environments more thoroughly, because the repeated loading accompanied by corrosion effects markedly reduce the lifetime of steel members<sup>1)-4)</sup>.

Steel bridge members are generally used with anticorrosion coatings. However, when a fatigue crack is once developed, even if coating materials are perfectly sound, coating layers are also cracked and fatigue crack surfaces would be exposed to corrosive environments of moisture, rainwater and/or salinity. Therefore, it is indispensable to take account of the effect of corrosive environments in evaluating the remaining life and setting the inspection period of fatigue damaged members.

Yazdani and Albrecht<sup>5)</sup> derived fatigue crack growth rate equations for structural

steels in air and in aqueous environments from over 3500 data points reported in literature. However, crack growth rate data in the long life region, which are essential in estimating the fatigue life of bridge members, have been scarcely obtained in aqueous environments. Komai et al<sup>6)</sup> tried to estimate the long-term corrosion fatigue crack growth curve in synthetic sea water using short-term crack growth data and corrosion pit growth rates.

Since most fatigue cracks in steel bridges have been found to originate in welded joints<sup>7)</sup>, it is necessary to obtain long-term corrosion fatigue crack growth equations under high tensile residual stresses introduced by welding. In this study, fatigue crack propagation tests are conducted in air and in the wet condition of 3% NaCl solution using plate-type specimens with longitudinal weldments in order to investigate the effect of corrosive environment on the long-term fatigue crack propagation behavior in welded members.

## 2. FATIGUE TEST METHOD

### (1) Specimen

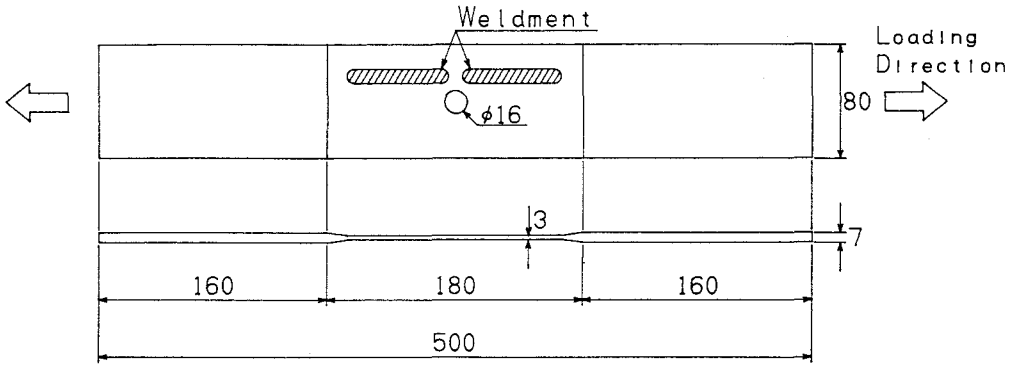
Fig.1 shows configurations and dimensions of the crack propagation specimen made of JIS SM570 steels, whose mechanical properties and chemical composition are given in Table 1. Quenched and tempered high strength steels are popularly used today in long span bridges constructed in seaside areas. A center hole is prepared to machine a pilot notch for pre-cracking.

Longitudinal weldments are beaded on both sides of the specimen for the purpose of

\* Member of JSCE, Dr. Eng., Assistant Professor, Dept. of Civil Eng., Kansai University (3-3-35, Yamate-cho, Suita, Osaka 564)

\*\* Member of JSCE, Dr. Eng., Professor, Dept. of Civil Eng., Ashikaga Institute of Technology

\*\*\* Member of JSCE, Kan-Den-Ko Co. Ltd.



(unit of length : mm)

Fig.1 Plate-type Specimen with Longitudinal Weldments.

Table 1 Mechanical Properties and Chemical Composition.

Material	Mechanical Properties			Chemical Composition (%)				
	Y.P. (MPa)	T.S. (MPa)	El. (%)	C ×100	Si ×100	Mn ×100	P ×1000	S ×1000
SM570	608	686	25	13	26	141	21	4

Table 2 Welding Conditions.

Current (A)	Voltage (V)	Welding Speed (cm/min)	Heat Input (kJ/cm)
120~130	22~23	30~40	4.0~6.0

introducing tensile residual stresses into the crack propagation area, considering the fact that fatigue crackings in steel bridges occur where high tensile residual stresses exist<sup>8)</sup>. Welding electrodes are JIS D5816, and welding conditions are given in Table 2.

Fig.2 shows distributions of longitudinal (perpendicular to the crack growth direction) residual stresses in the minimum cross section of a specimen measured by the cutting method and the redistribution behavior of them caused by the crack propagation. Plotted marks represent the average value of residual stresses on both sides of the specimen. High tensile residual stresses exist in the vicinity of the hole edge near welded beads before a fatigue crack is initiated, and also exist after crack initiation in front of the crack as a result of redistribution. Consequently, high tensile residual stresses exist in front of fatigue cracks at all times in crack propagation tests.

### (2) Corrosive environment

Steel bridges and other civil engineering structures are generally used in air and exposed to moisture, rain, and/or salinity supplied from sea water and antifreezing agents. The authors previously reported that salt water reduced the fatigue strength of structural steels more than distilled water and sulphurous solution of pH=4<sup>3)</sup>. Therefore, in this study, corrosion fatigue crack propagation tests are conducted in the wet condition of 3% NaCl solution (25±0.5°C, pH=7.1~7.2).

A corrosion chamber made of acrylic plastic is mounted to the specimen as shown in Fig.3. The solution is circulated at the flow rate of 1 l/min, and renewed every one week. The dissolved oxygen is saturated by aeration.

### (3) Loading condition

Fatigue crack propagation tests are conducted under tensile cyclic loading using an electro-hydraulic fatigue testing machine with the dynamic capacity of 98 kN.

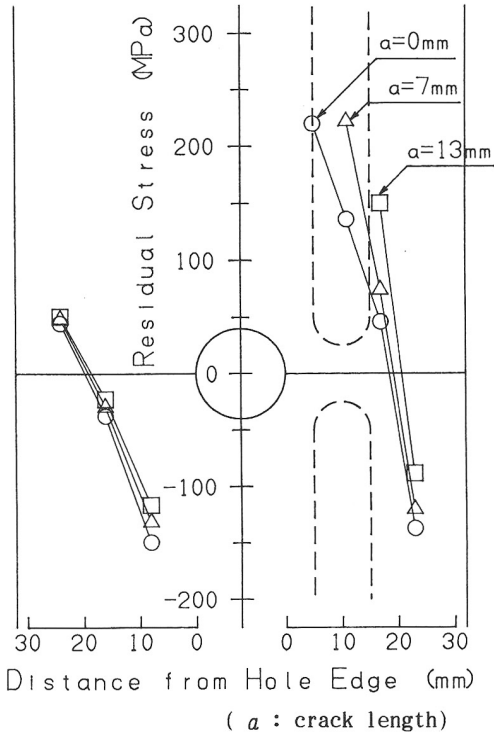


Fig. 2 Residual Stress Distributions.

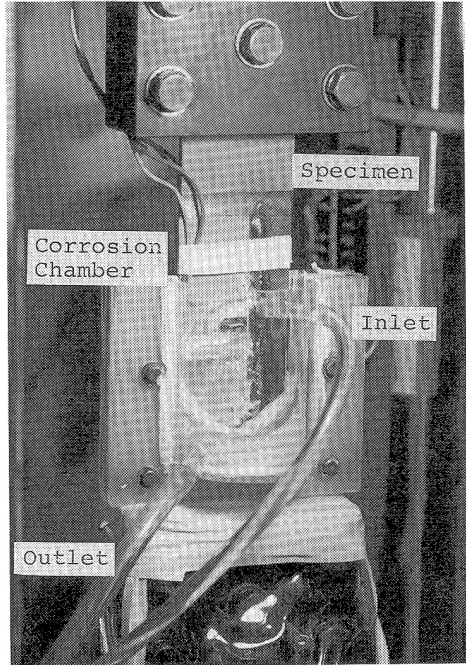


Fig. 3 Corrosion Fatigue Crack Propagation Test Set-up.

Considering a hypothesis that the long-term corrosion fatigue crack propagation could occur without crack closure phenomena<sup>6)</sup>, the maximum value of cyclic loading is fixed to be a constant of 18.6 kN (which corresponds to the net-section-based nominal stress of 95 MPa) for all specimens. The load range is reduced at the rate of 10~20% in  $\Delta K$ -decreasing tests, and increased at the rate of 10~30% in  $\Delta K$ -increasing tests.

The rate of stress repetition is set at 1 Hz in corrosion fatigue crack propagation tests considering that of the actual live loading in bridge members of relatively short span which are susceptible to fatigue damage<sup>3)</sup>. In air, fatigue crack propagation tests are performed at 10~20 Hz because the rate of stress repetition has little influence on the crack propagation behavior.

(4) Measurement of crack length

An alternating current potential method is applied to measuring the crack length in fatigue crack propagation tests. Fig. 4 illustrates the location of electric current input and potential probes. The

frequency of electric current is 50 Hz, and the effective value is 3.25 A. Fig. 5 shows the relationship between potential drop normalized by the maximum value and crack length from the notch tip obtained by beach mark tests in air. As shown in the figure, crack length is represented by a quadratic function of normalized potential drop. Crack propagation rates are calculated using the crack length data of 4~11 mm.

The stress intensity factor range  $\Delta K$  is expressed by Eq. (1).

$$\Delta K = S\gamma \cdot \sqrt{\pi a} \cdot F_g \cdot F_w \dots\dots\dots(1)$$

where  $S\gamma$  is the nominal stress range and  $a$  is the crack length.  $F_g$  is the correction factor for the effect of emanating from a circular hole, and  $F_w$  is that of the plate width and the eccentricity<sup>9)</sup>.  $F_w$  is calculated by Eq. (2).

$$F_w = \sqrt{\sec(\pi \lambda / 2) \cdot \sin(2 \lambda \epsilon) / (2 \lambda \epsilon)} \dots\dots\dots(2)$$

where  $\lambda = (d+a)/(w-a)$ ,  $\epsilon = a/w$ ,  $d$  is the diameter of circular hole, and  $w$  is the plate width.

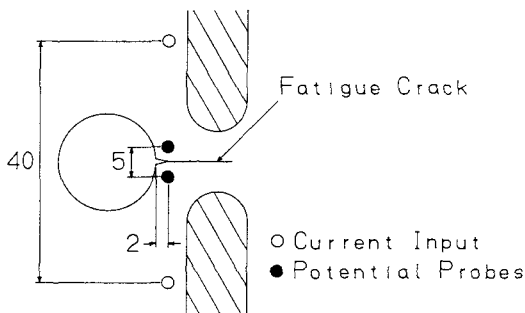


Fig.4 Location of Electric Contacts.  
 (unit of length : mm)

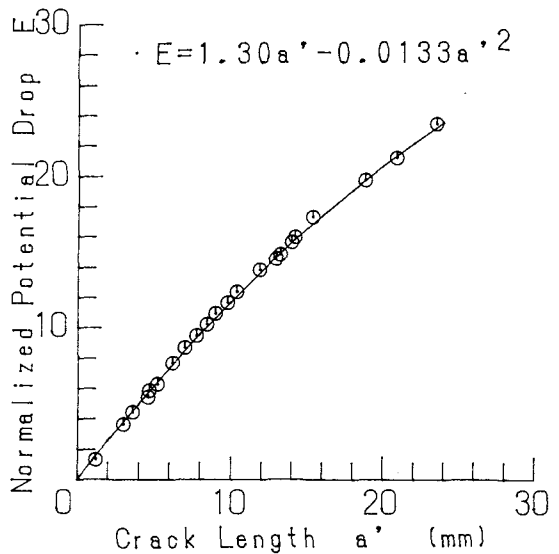


Fig.5 Relationship between Normalized Potential Drop and Crack Length.

Table 3 Fatigue Crack Propagation Test Results in air.

$\Delta N$ (cycles)	$a$ (mm)	$\Delta a$ (mm)	$\Delta P$ (kN)	$\Delta K$ (MPa $\sqrt{m}$ )	$da/dN$ (m/cycle)
$5.00 \times 10^4$	4.91	0.46	11.76	10.22	$9.20 \times 10^{-9}$
$5.00 \times 10^4$	5.12	0.21	9.80	8.62	$4.20 \times 10^{-9}$
$1.00 \times 10^5$	5.40	0.28	8.82	7.82	$2.80 \times 10^{-9}$
$1.00 \times 10^5$	5.65	0.25	7.84	7.01	$2.50 \times 10^{-9}$
$1.50 \times 10^5$	5.95	0.30	6.86	6.18	$2.00 \times 10^{-9}$
$3.00 \times 10^5$	6.33	0.38	5.88	5.35	$1.27 \times 10^{-9}$
$3.00 \times 10^5$	6.57	0.24	4.90	4.50	$8.00 \times 10^{-10}$
$4.00 \times 10^5$	6.71	0.14	4.31	3.98	$3.50 \times 10^{-10}$
$7.00 \times 10^5$	6.96	0.25	3.92	3.64	$3.57 \times 10^{-10}$
$1.00 \times 10^6$	7.10	0.14	3.53	3.29	$1.40 \times 10^{-10}$
$1.40 \times 10^6$	7.17	0.07	3.14	2.94	$5.00 \times 10^{-11}$
$1.04 \times 10^6$	7.31	0.14	3.33	3.13	$1.35 \times 10^{-10}$
$1.20 \times 10^6$	7.58	0.27	3.53	3.33	$2.25 \times 10^{-10}$
$3.00 \times 10^5$	8.01	0.43	5.88	5.68	$1.43 \times 10^{-9}$
$3.00 \times 10^5$	8.51	0.50	6.86	6.54	$1.67 \times 10^{-9}$

### 3. LONG-TERM CRACK PROPAGATION

#### (1) In air

Fatigue crack propagation test results in air are given in Table 3.  $\Delta N$  is the number of loading cycles for the increment of fatigue crack length  $\Delta a$  (i.e.  $\Delta a$  is the increment of fatigue crack length during  $\Delta N$  cycles), and  $\Delta P$  is the load range.  $\Delta K$  is the root-mean-cube value calculated by using  $a$  and  $(a - \Delta a)$ . The fatigue crack propagation rate  $da/dN$  is calculated as  $\Delta a / \Delta N$ .

Fig.6 shows the relationship between  $da/dN$

and  $\Delta K$  in air with the average and the most conservative design curves proposed in JSSC fatigue design recommendations<sup>10)</sup>. There is no difference between  $\Delta K$ -decreasing test results and  $\Delta K$ -increasing test results. Fatigue crack propagation rates obtained in air agree well with the JSSC average design curve, and a threshold stress intensity factor range of about 2.9 MPa $\sqrt{m}$  exists.

#### (2) In corrosive environment

Fatigue crack propagation test results in corrosive environment are given in Table 4. The fatigue crack is propagated when  $\Delta P =$

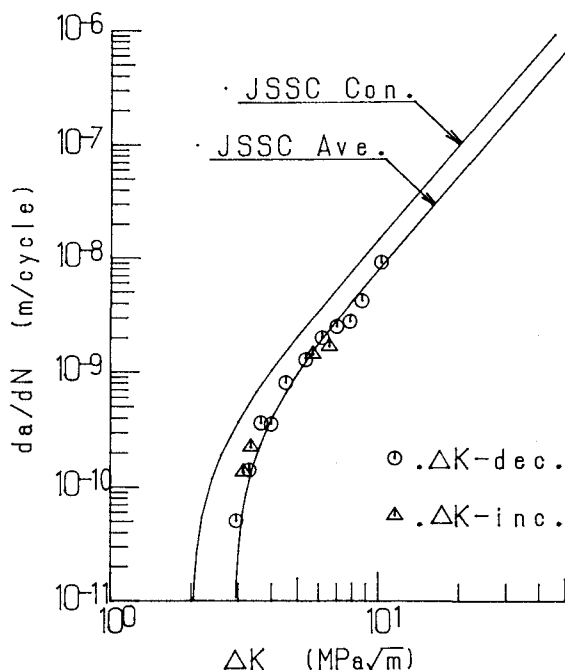


Fig.6 Crack Propagation Rates in Air.

0 but  $P = P_{max}$ . Contrastively, no crack growth can be detected when  $\Delta P = 0$  and  $P \approx 0$ . Fig.7 shows the relationship between  $da/dN$  and  $\Delta K$  in corrosive environment with JSSC design curves<sup>10)</sup>. There is no difference between  $\Delta K$ -decreasing test results and  $\Delta K$ -increasing test results.

As shown in Fig.7, fatigue crack propagation rates in corrosive environment agree well with the JSSC conservative design curve and are about twice as large as those in air in the region of  $\Delta K$  larger than the threshold value in air. However, the decreasing tendency of  $da/dN$  can not be observed and the value of  $da/dN$  is held to be almost constant in the smaller  $\Delta K$  region, even when  $\Delta P = 0$  so long as the absolute value of load is large enough to open the crack tip (see Table 4). Therefore, it should be considered that no threshold value exists in corrosive environment under high tensile residual stresses.

Fig.8 shows the comparison with corrosion fatigue crack propagation data of structural steels reported in literature. Iwasaki<sup>11)</sup> measured fatigue crack growth rates of 800MPa-class high strength steels in seawater with frequency of 0.17 Hz and stress ratio of 0.0~0.1. Matsuoka et al.<sup>12)</sup> measured those of the similar steel in

synthetic seawater and 3% NaCl solution with frequency of 30~50 Hz and stress ratio of 0.5~0.95. Both data reported by them demonstrate the threshold behavior because of the absence of high tensile residual stresses (Iwasaki's data) and because of the too high frequency (Matsuoka's data). It must be remarked that no threshold value exists against the corrosion fatigue crack propagation in welded bridge members.

### (3) Proposed propagation rate equations

Since corrosion fatigue crack propagation data agree well with the JSSC conservative design curve in the region of  $\Delta K$  larger than the threshold value in air and the value of  $da/dN$  is almost constant in the smaller  $\Delta K$  region, the relationship between  $da/dN$  and  $\Delta K$  of welded members in corrosive environment can be represented by two straight lines as shown in Fig.8 and expressed by Eqs. (3) and (4).

$$da/dN = 2.7 \times 10^{-11} \cdot \Delta K^{2.75} \quad (\Delta K \geq 2.7 \text{ MPa}\sqrt{\text{m}}) \quad \text{----(3)}$$

$$da/dN = 4.0 \times 10^{-10} \quad (\Delta K < 2.7 \text{ MPa}\sqrt{\text{m}}) \quad \text{----(4)}$$

The constant value of  $4.0 \times 10^{-10}$  m/cycle is almost equivalent to corrosion pit growth rates at stress-concentrated portions in several structural steels under cyclic loading reported by the authors<sup>3), 4)</sup>.

Table 4 Fatigue Crack Propagation Test Results in corrosive environment.

$\Delta N$ (cycles)	$a$ (mm)	$\Delta a$ (mm)	$\Delta P$ (kN)	$\Delta K$ (MPa $\sqrt{m}$ )	$da/dN$ (m/cycle)
$5.00 \times 10^3$	4.38	0.29	17.64	15.08	$5.80 \times 10^{-8}$
$5.00 \times 10^3$	4.53	0.15	15.68	13.52	$3.00 \times 10^{-8}$
$8.00 \times 10^3$	4.81	0.28	15.68	13.62	$3.50 \times 10^{-8}$
$1.50 \times 10^4$	5.18	0.37	13.72	12.05	$2.47 \times 10^{-8}$
$1.90 \times 10^4$	5.48	0.30	11.76	10.45	$1.58 \times 10^{-8}$
$3.50 \times 10^4$	5.86	0.38	9.80	8.80	$1.09 \times 10^{-8}$
$6.50 \times 10^4$	6.24	0.38	7.84	7.12	$5.85 \times 10^{-9}$
$8.00 \times 10^4$	6.63	0.39	6.86	6.30	$4.88 \times 10^{-9}$
$1.60 \times 10^5$	7.25	0.62	5.88	5.48	$3.88 \times 10^{-9}$
$1.48 \times 10^5$	7.49	0.24	4.90	4.62	$1.62 \times 10^{-9}$
$1.00 \times 10^5$	7.73	0.24	5.88	5.58	$2.40 \times 10^{-9}$
$2.60 \times 10^5$	8.12	0.39	4.90	4.69	$1.50 \times 10^{-9}$
$5.00 \times 10^5$	8.37	0.25	3.92	3.78	$7.40 \times 10^{-10}$
$7.40 \times 10^5$	8.63	0.26	3.14	3.05	$3.51 \times 10^{-10}$
$8.60 \times 10^5$	8.98	0.35	2.74	2.69	$4.07 \times 10^{-10}$
$4.30 \times 10^5$	9.11	0.13	2.35	2.32	$3.02 \times 10^{-10}$
$4.50 \times 10^5$	9.31	0.20	1.96	1.94	$4.44 \times 10^{-10}$
$5.00 \times 10^5$	9.51	0.20	1.76	1.76	$4.00 \times 10^{-10}$
$5.60 \times 10^5$	9.72	0.21	1.57	1.57	$3.75 \times 10^{-10}$
$2.35 \times 10^5$	9.82	0.10	1.37	1.38	$4.26 \times 10^{-10}$
$4.90 \times 10^5$	10.01	0.19	0.00*	0.00*	$3.88 \times 10^{-10}$
$5.70 \times 10^5$	10.01	<0.01	0.00**	0.00**	$<1.8 \times 10^{-11}$
$2.24 \times 10^5$	10.11	0.10	2.94	2.98	$4.46 \times 10^{-10}$
$1.70 \times 10^5$	10.31	0.20	3.92	3.99	$1.18 \times 10^{-9}$
$1.10 \times 10^5$	10.54	0.23	4.90	5.01	$2.09 \times 10^{-9}$
$4.30 \times 10^4$	10.67	0.13	5.88	6.04	$3.02 \times 10^{-9}$

\* )  $P=18.62\text{kN}(=P_{max})$ ,  $K=18.8\text{MPa}\sqrt{m}$ ; \*\* )  $P=0.98\text{kN}$ ,  $K=0.99\text{MPa}\sqrt{m}$

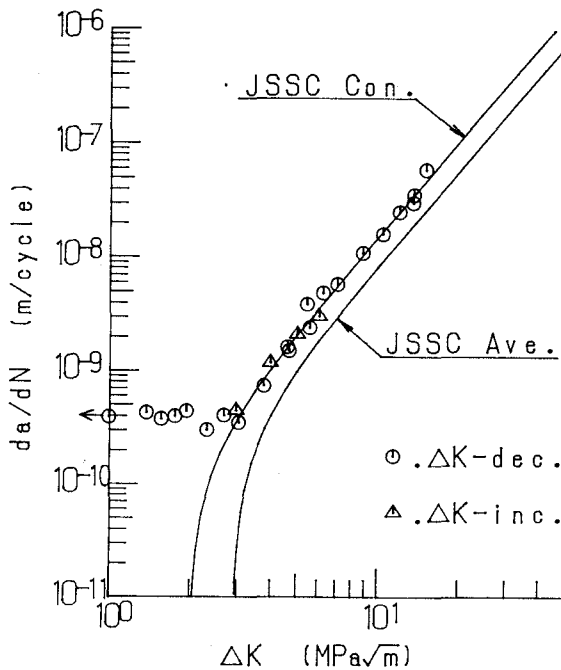


Fig.7 Crack Propagation Rates in Corrosive Environment.

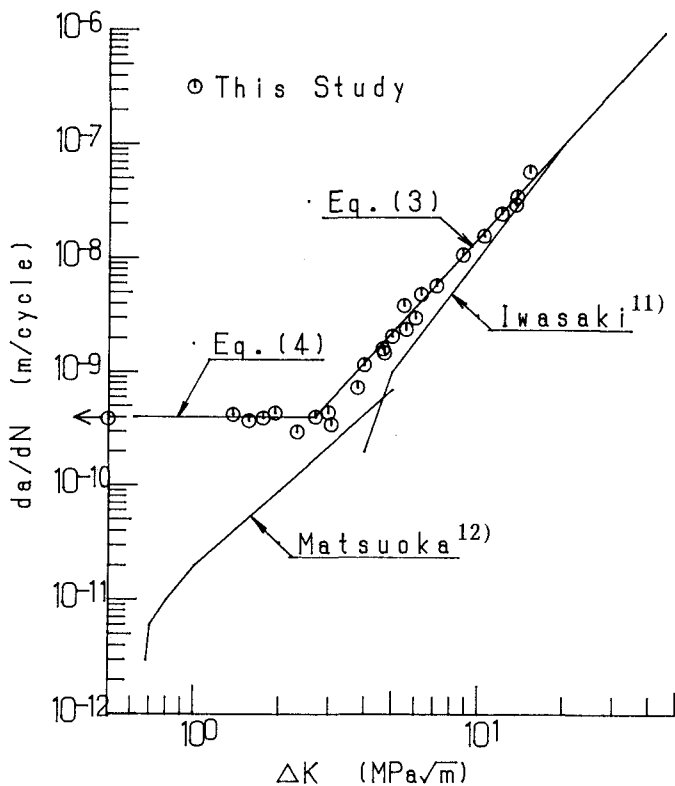


Fig.8 Comparison of Corrosion Fatigue Crack Propagation Rates with the Data in Literature.

#### 4. CONCLUDING REMARKS

Long-term fatigue crack propagation tests are performed in air and in the wet condition of 3% NaCl solution using welded plate specimens with high tensile residual stresses in front of the fatigue crack. The following are the principal results obtained from this study.

(1) Fatigue crack propagation rates obtained in air agree well with the JSSC average design curve, and a threshold stress intensity factor range of about  $2.9 MPa\sqrt{m}$  exists.

(2) Fatigue crack propagation rates in corrosive environment agree well with the JSSC conservative design curve in the region of  $\Delta K$  larger than the threshold value in air. However, in the smaller  $\Delta K$  region, no threshold behavior can be observed and the crack propagation rate is held to be almost constant even when the load range equals zero so long as the absolute value of load is large enough to open the crack tip.

(3) The relationship between  $da/dN$  and  $\Delta K$

of welded members in corrosive environment can be represented by the JSSC conservative design curve in the region of  $\Delta K$  larger than the threshold value in air and by the constant value in the smaller  $\Delta K$  region.

#### ACKNOWLEDGMENT

The authors would like to thank Prof. Ichizou Mikami of Kansai University for his invaluable advice and suggestion. This study was supported in part by the Grant-in-Aid for Encouragement of Young Scientists from the Japanese Ministry of Education, Science and Culture (No.01750428).

#### REFERENCES

- 1) Nishimura, A. and Minata, O. : Surface Irregularity and Fatigue Strength of Gusset Joint under Various Corrosive Environments, Proc. of JSCE, No.380/I-7, pp.401-409, 1987 (in Japanese).
- 2) Yamada, K. and Sadaka, S. : Fatigue Test of Stiffener Specimens in Salt Water and Life Estimation, Proc. of JSCE, No.398/I-10, pp.377-384, 1988 (in

- Japanese).
- 3) Sakano, M., Yokoh, M., Arai, H. and Nishimura, T. : Fatigue Crack Initiation Life of Notched Steel Members in Corrosive Environments, Journal of Structural Engineering, Vol.34A, pp.469-481, 1988 (in Japanese).
  - 4) Sakano, M., Arai, H. and Nishimura, T. : Long Life Fatigue Behavior of Fillet Welded Joint in Corrosive Environment, Structural Eng./ Earthquake Eng., Vol.6, No.2, pp.365s-373s, 1989.
  - 5) Yazdani, N. and Albrecht, P. : Crack Growth Rates of Structural Steel in Air and Aqueous Environments, Engineering Fracture Mechanics, Vol.32, No.6, pp.997-1007, 1989.
  - 6) Komai, K., Minoshima, K. and Kim, G. : An Estimation Method of Long-Term Corrosion Fatigue Crack Growth Characteristics, Trans. JSME, Vol.54, No. 499, pp.509-512, 1988 (in Japanese).
  - 7) Miki, C. and Sakano, M : A Survey of Fatigue Cracking Experience in Steel Bridges, Technical Report, No.39, Dept. of Civil Eng., Tokyo Institute of Technology, pp.33-45, 1988.
  - 8) Sakano, M., Furukawa, M., Takenouchi, H. and Nishimura, T. : Measurements of Welding Residual Stresses in Steel Bridges, Bridge and Foundation Engineering, Vol.20, No.3, pp.27-30, 1986 (in Japanese).
  - 9) Ishida, M. : Elastic Analyses of Cracks and Stress Intensity Factors, Baifukan, 1976 (in Japanese).
  - 10) The Society of Steel Construction of Japan : Recommendations for Fatigue Design, JSSC Report No.14, 1989 (in Japanese).
  - 11) Iwasaki, N. : Study on Corrosion Fatigue Strength in Sea Water of Structural Steels and Joints, Doctoral Thesis, Osaka University, 1987 (in Japanese).
  - 12) Matsuoka, S. et al. : Threshold Behavior of Fatigue Crack Growth in Synthetic Seawater, J. of Iron and Steel Institute of Japan, Vol.72, No.12, p.406, 1986 (in Japanese).

(Received April 3, 1991)

## 溶接部材の長寿命腐食疲労亀裂進展特性

坂野昌弘・西村俊夫・木暮 健

溶接部材の長寿命疲労亀裂進展挙動に及ぼす腐食環境の影響を検討することを目的として、縦方向溶接部をもつ平板試験体を用いて空気中および3%食塩水による濡れ環境下における疲労亀裂進展実験を行った。腐食環境下では、疲労亀裂は低 $\Delta K$ 領域においても進展し、亀裂進展の下限界値( $\Delta K_{th}$ )の存在は認められなかった。空気中の $\Delta K_{th}$ 以下の領域では、腐食疲労亀裂進展速度はほぼ一定値で表すことができる。